

The refinement of zinnwaldite-1M in subgroup symmetry

STEPHEN GUGGENHEIM¹ AND S. W. BAILEY

Department of Geology and Geophysics, University of Wisconsin
Madison, Wisconsin 53706

Abstract

The structure of a zinnwaldite-1M from the Sadisdorf Mine, D.D.R., has been refined in $C2/m$, $C2$, and $C1$ symmetries. The composition is $(K_{0.90}Na_{0.05})(Al_{1.05}Fe_{0.16}^{3+}Ti_{0.01}Fe_{0.77}^{2+}Mn_{0.05}Mg_{0.01}Li_{0.67})(Si_{3.09}Al_{0.91})O_{10}(OH)_{0.79}F_{1.21}$. The cell parameters are $a = 5.296$, $b = 9.140$, $c = 10.096$ Å, and $\beta = 100.83^\circ$. Refinement in triclinic symmetry $C1$ using the ordered-model approach gave atomic coordinates consistent with monoclinic $C2$ symmetry. In $C2$ symmetry, octahedra $M(2)$ and $M(3)$ related by the pseudo-mirror plane are significantly different in size (mean $M-O, F = 1.882, 2.131$ Å) and, to a lesser extent, in electron count (11.5 and 13.5). Octahedral Al completely occupies $M(2)$, and the remaining Fe, Li, other cations, and vacancies are nearly randomly distributed over $M(3)$ and the *trans* octahedron $M(1)$. The (F,OH) atom has moved off the pseudo-mirror plane in order to coordinate more closely with Al in $M(2)$. It is anticipated that all fluorine-rich zinnwaldites and lepidolites will have a similar ordering pattern. The *cis*-orientation of fluorine along the $M(2):M(3)$ shared edge allows a closer F—F approach around a small cation in either site than is possible along any $M(1)$ shared edge involving larger oxygen atoms. The larger $M(1)$ and $M(3)$ octahedra are flattened considerably ($\psi = 60.8^\circ$) in order to fit onto the smaller, more regular ($\psi = 56.5^\circ$) $M(2)$ octahedron. The two nonequivalent tetrahedra differ slightly in size (mean $T-O = 1.646, 1.639$ Å), are elongate, and rotated by 5.8° .

Introduction

Zinnwaldite is a Li,Fe,Al trioctahedral mica commonly found in greisens, associated veins, and in some granites and pegmatites. It is defined by Foster (1960) as having a Li content of 1.00 ± 0.25 atoms per formula unit (~ 2.50 – 4.50 weight percent Li_2O), in contrast to protolithionite with 0.50 ± 0.25 atoms and lepidolite with > 1.25 atoms. Rieder (1968, 1970a) and Rieder *et al.* (1971) have studied a suite of natural Li-Fe micas, from the Krušné hory Mountains (Erzgebirge) of Czechoslovakia and Germany, that lie close to the join between polyolithionite and siderophyllite. As a result of this study Rieder (1970a) proposed broadening the composition of zinnwaldite so that it ranges from $x = 1$ to 3 in the series $K_2Fe_x^{2+}Li_{4-x}(Al,Fe^{3+})_2(Al_xSi_{8-x})O_{20}(OH,F)_4$, where $x = 0$ for polyolithionite and $x = 4$ for siderophyllite. Most of the zinnwaldites were of the 1M structural type (Rieder, 1970b).

Rieder (1968) agrees with Foster (1960) that there always is close to 1.0 small trivalent octahedral cation

(Al,Fe³⁺) per formula unit in zinnwaldite. Although the larger octahedral cations (Li,Fe²⁺,Mg,Mn) are somewhat variable in number, they never exceed 2.0. This ideal ratio of 1:2 led Rieder to postulate octahedral ordering for zinnwaldite-1M of the type found in clintonite-1M (= xanthophyllite), wherein each small $M(1)$ octahedron on the mirror plane of the ideal $C2/m$ space group is surrounded symmetrically by six larger $M(2)$ octahedra in an overall 1:2 ratio. This ordering was believed to account for the observation that $d(001)$ values for natural zinnwaldites are about 0.1 Å smaller than for synthetic specimens, which are presumed to be disordered.

Approximately two dozen mica structures have been refined that show octahedral ordering, either of cations or, for dioctahedral compositions, of cations plus vacancies. Clintonite-1M (= xanthophyllite) is the only exception to the rule that the unique octahedron $M(1)$ on the symmetry plane of each layer is larger than the two equivalent $M(2)$ octahedra. The "normal" ordering pattern with $M(1)$ larger than the average $M(2)$ site has been shown to be adopted even in cases where the octahedral composition logically might suggest the reverse pattern. An example is

¹ Present address: Dept of Geological Sciences, University of Illinois at Chicago Circle, Box 4348, Chicago, Illinois 60680.

polyolithionite-1*M*, in which there are two large octahedral Li ions and one smaller Al ion. However, the ordering pattern found by Takeda and Burnham (1969) consists of one large *M*(1) octahedral site on the mirror plane with composition $\text{Li}_{0.89}\text{Al}_{0.11}$ and two smaller symmetry-related *M*(2) sites of average composition $\text{Li}_{0.55}\text{Al}_{0.45}$.

This paper reports an X-ray refinement of one of Rieder's zinnwaldite specimens. This study was undertaken, first, to test the Rieder ordering hypothesis, because it would be of particular interest to find another exception to the prevalent ordering pattern. Second, even if the "normal" ordering pattern were to be found, the composition appears so favorable for ordering that the possibility of crystallographically-distinct *M*(2) sites should be investigated in subgroup symmetry. Refinement in subgroup symmetry has not been attempted often, but recently has been successful in showing tetrahedral ordering in margarite-2*M*₁ (Guggenheim and Bailey, 1975) and both tetrahedral and octahedral ordering in a dioctahedral 1*M* mica (Sidorenko *et al.*, 1975).

Experimental

Dr. Milan Rieder of Charles University kindly furnished a suite of analyzed zinnwaldite samples. A crystal from sample #40 from the Sadisdorf Mine dump, D.D.R., was selected as giving the sharpest reflections. The crystal is $0.4 \times 0.3 \times 0.05$ mm and light amber in color. The composition of the crystal used for the structural analysis was determined by electron microprobe analysis (Table 1) after the completion of data collection. The Li content and the ratio of Fe^{2+} to Fe^{3+} were taken from the wet-chemical analysis data for the bulk sample as reported by Rieder (1970*a*). The resulting formula unit is $(\text{K}_{0.90}\text{Na}_{0.05})(\text{Al}_{1.05}\text{Fe}_{0.16}^{3+}\text{Ti}_{0.01}\text{Fe}_{0.77}^{2+}\text{Mn}_{0.05}\text{Mg}_{0.01}\text{Li}_{0.67}\square_{0.28})(\text{Si}_{3.09}\text{Al}_{0.91})\text{O}_{10}(\text{OH})_{0.79}\text{F}_{1.21}$. This formula is similar to that given by the bulk analysis, except for a slightly lower Si content. Rieder *et al.* (1971) cite $2V_{\alpha} = 27^{\circ} \pm 1^{\circ}$ and the γ refractive index as 1.595 \pm 0.001 for this specimen.

Unit-cell parameters of $a = 5.296(1)$, $b = 9.140(2)$, $c = 10.096(3)$ Å, and $\beta = 100.83(2)^{\circ}$ were determined by least-squares refinement of 15 high-angle reflections measured on a Syntex P2₁ autodiffractometer. Two intensity data sets were collected. First, the intensities of 2,993 non-zero reflections were measured, using graphite-monochromatized $\text{MoK}\alpha$ radiation. The data were collected in the $2\theta:\theta$ variable-scan mode in four quadrants of the limiting sphere from $2^{\circ} < 2\theta < 90^{\circ}$. Two standard reflections were mon-

Table 1. Chemical analysis of Sadisdorf zinnwaldite

Oxide	^a Wet	Weight percent		Cations per 22 positive charges		
		Microprobe	Best data			
SiO ₂	42.86	40.70	40.70	Si	3.090	4.000 ^{IV}
Al ₂ O ₃	21.89	21.95	21.95	Al	0.910	
TiO ₂	0.16	0.20	0.20		1.054	
Fe ₂ O ₃	2.78	15.04	12.19	Ti	0.011	2.721 ^{VI}
FeO	11.84			Fe ³⁺	0.163	
MnO	0.73	0.70	0.70	Fe ²⁺	0.774	
MgO	^b tr	0.04	0.04	Mn	0.045	
Li ₂ O	2.19	^c na	2.19	Mg	0.005	
CaO	0.51	^d bd	0.00	Li	0.669	
Na ₂ O	0.26	0.36	0.36	Na	0.053	0.953 ^{XII}
K ₂ O	9.85	9.29	9.29	K	0.900	
P ₂ O ₅	0.04	na	0.00			
H ₂ O ⁺	na	na	na			
H ₂ O ⁻	0.96	na	0.96			
F ⁻	5.20	5.67	5.67			
Sum of Oxides	99.27	93.95	97.10			

^aWet chemical analysis by M. Huka and J. Obermajer, Geological Survey of Czechoslovakia, as reported by Rieder (1970*a*).
^bTrace. ^cNot analyzed. ^dBelow detection.

itored after every 50 reflections to check crystal and electronic stability. Reflections were considered as observed if $I > 2\sigma(I)$, where I was calculated from $I = [S - (B_1 + B_2)/B_r]T_r$, S being the scan count, B_1 and B_2 the background, B_r the ratio of background time to scan time, and T_r the 2θ scan rate in degrees per minute. $\sigma(I)$ was calculated from standard counting statistics. Integrated intensities were corrected for Lorentz and polarization effects, but not for absorption. This data set was used for initial refinement and for determining the best ordering models in both monoclinic and triclinic subgroup symmetry. Final refinement of the monoclinic models used a second data set of 1,550 independent non-zero intensities collected in the same manner from only two quadrants. These data were empirically corrected for absorption by comparing the data to complete ψ scans (10° increments in ϕ) for selected reflections spaced at 2θ intervals of 5° . Absorption is a major factor because of the platy nature of the crystal. A maximum intensity decrease of 49 percent was observed for some reflections during the ψ scans.

Refinement

Initial atomic coordinates in the ideal space group $C2/m$ were obtained from the structure of fluor-polyolithionite (Takeda and Burnham, 1969). After several cycles of least-squares refinement with program ORFLS using the first data set with reflections from $2^{\circ} < 2\theta < 55^{\circ}$, scattering-factor adjustments to *M*(1) and *M*(2) were made as a result of three-dimensional electron-density difference maps. Additional least-squares refinement reduced R_1 to 12.5 percent. At this stage *M*(1) was significantly larger than *M*(2), and

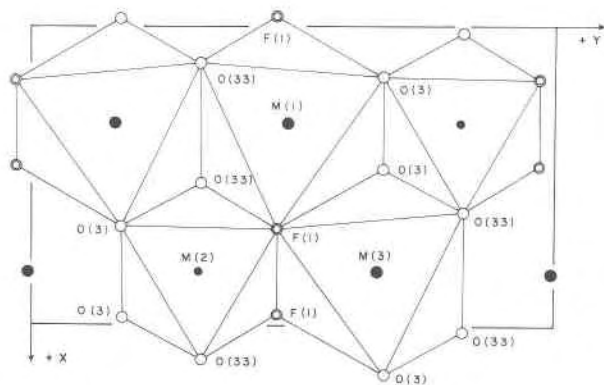


Fig. 1. Octahedral ordering pattern of Sadisdorf zinnwaldite-1M in subgroup C_2 .

the average (F,OH) atom had an unusually high temperature factor of 3.0 \AA^2 . This is the "normal" ordering pattern, so subsequent refinement concentrated on subgroup ordering models.

Refinement in subgroup symmetry initially followed the method outlined by Guggenheim and Bailey (1975) for margarite-2 M_1 . Because of convergence problems, it is best not to start refinement in subgroup symmetry by using atomic coordinates of higher symmetry. Instead, atoms were moved away from their pseudosymmetrically-related positions by postulating an ordering scheme in subgroup symmetry that was still consistent with the parent space-group refinement. The atomic coordinates of each possible ordering model were determined from a distance-least-squares program, and those results were then refined by varying the parameters of pseudosymmetry-related positions independently. The latter precaution actually may not be necessary, since in the later stages of refinement it proved possible to vary all of the parameters together without significantly high correlations.

For subgroup C_2 , the $M(2)$ site and its pseudosymmetrically-related $M(3)$ site become crystallographically independent (Fig. 1). Three-dimensional electron-density difference maps at this stage indicated $M(3)$ had approximately four more electrons per site than $M(2)$. Only two ordered models are compatible with the average structure in the parent space group C_2/m , namely $M(2)$ can be smaller or larger than $M(3)$. Atomic coordinates for these two models were derived, using the DLS program OPTDIS written by W. A. Dollase of the University of California at Los Angeles. Subsequent cycles of ORFLS refinement indicated the model with $M(2)$ smaller than $M(3)$ to be much better than the reverse model ($wR = 8.9\%$ versus 14.0%).

There is only one independent tetrahedral site in the parent space group C_2/m . Although there are two independent tetrahedra in space group C_2 , mean $T-O$ distances for both proved to differ by only 0.01 \AA , so that any ordering of Si,Al must be very small. The twofold axis passing through the 2:1 layer in space group C_2 relates tetrahedra on one side of the octahedral sheet to tetrahedra on the other side. It is implicit in space group C_2 , therefore, that both tetrahedral sheets must be identical. To determine whether tetrahedral ordering is present in still lower symmetry or whether both tetrahedral sheets are the same in composition, four models representing all possible tetrahedral ordering patterns were postulated for triclinic C_1 symmetry. The four models were tested with the four-quadrant intensity data of set one, and each converged back from the postulated ordered atomic coordinates to the more disordered structure of C_2 symmetry with equivalent tetrahedral sheets. For all refinements involving noncentrosymmetric space groups, one atom was fixed in position.

Final refinement of the best C_2 model and of the C_2/m average structure was accomplished with the second data set in two stages, first using only 633 independent reflections with $2\theta \leq 55^\circ$ from two quadrants and incorporating absorption corrections. Initially, pseudosymmetry-related atomic coordinates were varied independently in two sets until the final stages of refinement. Then a full matrix refinement was used. No significant differences in atomic positions resulted from this refinement relative to that using the first data set, so final refinement consisted primarily of adjustment of isotropic temperature factors (B) and of scattering factors (f) for the octahedral cations, as determined by alternating cycles of electron-density difference maps and least-squares refinement. The f and B values proved interrelated in that an increase of one electron in octahedral scattering power would increase B for that same site by approximately 0.25 , and the reverse for a decrease. Refinement was terminated for both models when f values that gave flat difference maps also satisfied the total octahedral-site composition for half-ionized atoms and were correlated with reasonable isotropic B values. Unweighted R for the isotropic C_2 ordered model was 6.1 percent and for the average C_2/m structure was 12.2 percent at this stage. In the second stage of final refinement, both the C_2 ordered model and the C_2/m average structure were refined with anisotropic temperature factors, using the second data set out to $2\theta \leq 90^\circ$. Fifty-seven reflections known to be associated with strong white-

Table 2. continued.

H	K	IOFO	IOFC	H	K	IOFO	IOFC	H	K	IOFO	IOFC	H	K	IOFO	IOFC		
3	13	78	103	-2	6	197	208	3	5	92	67	L	16				
-5	13	113	108	-4	6	84	70	-3	5	86	94						
1	15	222	244	8	110	107		-5	5	174	150			0	93	98	
-1	15	274	298	1	7	165	157	0	6	148	142			2	0	111	114
-3	15	177	197	-1	7	110	104	-2	6	98	98			4	0	108	291
-2	16	86	75	1	7	108	84	-2	6	85	80			-4	0	128	138
				-3	7	102	107	4	6	135	138			-1	1	93	98
				5	7	70	76	-4	6	292	310			-3	1	116	114
L	10			-7	7	98	71	-6	6	250	262			-5	1	61	67
				0	8	274	270	-8	6	109	99			-7	1	87	76
-4	0	394	392	-2	8	179	158	-1	7	105	83			4	2	82	63
6	0	127	110	-2	8	95	106	-3	7	132	123			4	2	82	63
-6	0	337	297	-8	8	65	51	5	7	105	83			-4	2	142	111
8	0	236	245	1	9	139	125	-5	7	80	89			1	3	201	202
-8	0	120	113	-1	9	63	72	-7	7	103	107			-1	3	219	223
1	1	177	177	3	9	139	122	0	8	95	88			-3	3	172	161
-1	1	86	84	-3	9	205	203	8	8	189	187			-5	3	95	86
3	1	180	197	5	9	279	274	-6	8	121	116			0	4	62	52
-3	1	59	63	-5	9	259	264	1	9	333	343			-2	4	147	137
1	1	112	117	-7	9	272	273	-1	9	376	338			-4	4	66	55
-5	1	87	102	0	10	144	144	-2	10	195	195			-7	4	61	54
7	1	76	63	-2	10	131	133	-3	9	100	93			-3	5	95	100
-7	1	84	71	-2	10	79	60	0	10	86	88			7	6	115	110
-9	1	137	124	-6	10	101	92	-6	10	106	102			-2	6	66	65
0	2	155	165	4	11	192	186	1	11	88	95			-4	6	81	97
2	2	273	261	-5	11	71	20	-1	11	103	101			-8	6	116	127
-2	2	152	156	0	12	256	258	3	11	67	70			3	7	85	85
4	2	92	92	2	12	192	187	-2	11	105	105			-7	8	104	54
-4	2	81	67	-2	12	125	143	0	12	129	130			-2	8	84	66
-8	2	91	88	-4	12	75	77	2	12	74	68			1	9	170	170
1	3	195	195	-6	12	66	61	-4	12	173	166			-1	9	170	159
3	3	512	525	0	13	144	144							9	13	131	131
-3	3	100	103	-1	13	108	120							-5	9	110	107
5	3	273	300	0	14	174	170							0	10	85	79
-5	3	73	76	2	14	137	144							-4	10	101	76
-7	3	100	112					2	0	128	119						
-9	3	199	193					2	0	381	381						
0	4	58	58	L	12			-2	0	436	435						
2	4	209	202					-6	0	68	81			L	17		
-2	4	83	88	2	0	559	564	1	1	115	93			2	0	127	114
4	4	181	184	-2	0	152	151	-1	1	54	48			-2	0	180	176
-4	4	184	181	4	0	351	365	3	1	138	136			-4	0	251	236
6	4	82	71	-4	0	56	47	-3	1	85	92			-6	0	115	108
-8	4	164	157	6	0	131	134	5	1	96	97			3	1	81	76
8	4	116	106	-6	0	356	320	0	1	95	110			-4	1	86	74
-1	5	73	74	-8	0	242	226	-2	1	94	98			-1	1	83	69
3	5	213	224	1	1	54	47	-4	2	104	97			-4	2	99	96
5	5	79	88	-1	1	120	124	-4	2	106	116			1	3	293	276
-5	5	98	88	3	1	104	98	-1	2	150	141			-3	3	104	68
7	5	91	81	-3	1	121	121	-8	2	87	87			3	3	231	225
-9	5	108	106	5	1	71	56	3	3	174	176			4	4	64	56
0	6	404	412	-5	1	70	67	3	3	153	144			-6	4	93	74
2	6	70	87	0	2	70	66	-3	3	159	144			3	3	93	77
-2	6	389	374	-2	2	297	312	5	3	144	137			0	6	65	55
6	6	89	94	-4	2	177	177	-7	3	185	199			-2	6	139	138
-4	6	440	455	3	3	480	498	-2	4	106	106			-2	6	190	170
6	6	165	180	3	3	187	168	-2	4	130	110			-4	6	170	165
-6	6	246	236	-3	3	486	514	4	4	68	57			-6	6	153	154
1	7	152	148	3	3	228	216	4	4	91	84			-3	7	106	87
-1	7	65	61	-7	3	60	36	-8	4	84	88			-5	7	81	72
3	7	101	101	0	4	210	219	1	5	129	114			-2	8	103	95
-3	7	93	95	2	4	70	56	3	5	131	116			-1	9	104	91
5	7	76	79	-2	4	179	199	-3	5	83	85						
-9	7	80	77	4	4	75	58	5	5	73	80						
0	8	74	65	-4	4	180	164	-7	5	75	74			L	18		
2	8	175	147	-6	4	143	124	0	6	150	89			-2	0	291	282
4	8	221	205	-1	5	167	165	-2	6	388	366			-4	0	85	98
-4	8	135	122	3	5	133	124	-4	6	294	297			-1	1	90	88
6	8	60	67	-3	5	118	112	-6	6	129	134			0	2	75	70
1	9	260	238	4	6	181	174	4	7	105	115			2	2	78	53
-1	9	69	83	4	6	314	313	-3	7	101	90			-2	2	76	23
3	9	370	336	-4	6	67	72	0	8	60	51			-1	3	110	98
9	9	128	119	3	7	182	173	1	9	96	103			-3	3	60	26
5	9	207	199	-8	6	257	255	1	9	78	84			-5	3	191	168
-5	9	70	90	1	7	80	75	-1	9	78	84			-1	5	68	41
-3	1	94	98	-1	7	78	85	3	9	101	116			-1	5	87	89
0	10	111	100	-3	7	147	145	4	9	116	144			0	6	239	233
2	10	158	149	0	8	145	143	-2	10	77	41			-2	8	798	771
4	10	83	103	2	8	120	119	-4	10	78	62			-4	6	99	102
1	11	92	83	-1	8	102	104	0	11	104	99			-1	7	84	76
3	11	145	140	-8	8	104	114	-1	11	85	44						
0	12	175	175	-8	8	66	43	-3	11	134	108						
-2	12	62	51	1	9	61	51	-1	12	104	99						
-4	12	259	272	-1	9	306	306	-2	12	206	227						
-4	12	247	253	-3	9	397	392	-4	12	203	211						
-6	12	164	178	-5	9	143	149	-5	13	180	159						
2	14	80	76	-1	9	62	44	-1	13	180	159						
-1	15	114	127	0	10	76	73	L	15					-4	0	134	110
-1	15	93	80	-2	10	184	187	-5	0	206	199			-5	1	83	77
				-1	11	106	116	2	0	177	169			-1	1	71	56
				-4	10	149	153	-2	0	161	174			-3	3	251	230
				-6	10	65	53	4	0	161	174			0	4	91	54
L	11			1	11	81	97	1	1	151	144						
2	0	466	470	-1	11	106	116	-1	1	168	148						
-2	0	155	154	-3	11	148	161	3	1	86	88						
0	122	124	0	0	12	152	155	-5	1	78	66						
-4	0	59	61	2	12	260	271	0	2	151	138						
6	0	122	119	0	14	84	52	2	2	70	50						
-6	0	94	85	-2	14	169	182	-4	2	111	100						
1	1	165	171					1	3	121	112						
-1	1	193	184					-3	3	206	186						
3	1	62	23					3	3	98	99						
-3	1	94	98					5	3	310	324						
0	2	235	232	4													

Table 3. Final atomic parameters

Atom	x	y	z	$B_{\text{equiv.}}$	β_{11}	β_{22}	β_{33}	β_{12}	β_{13}	β_{23}
K(1)	0	0.5028(2)	0	1.93	0.0181(4)	0.0048(1)	0.0054(1)	0.0	0.0013(2)	0.0
M(1)	0	-0.0069(3)	1/2	0.64	0.0067(3)	0.0009(1)	0.00236(8)	0.0	0.0013(1)	0.0
M(2)	0	0.3217(3)	1/2	0.57	0.0050(4)	0.0014(1)	0.0017(1)	0.0	0.0006(2)	0.0
M(3)	1/2	0.1631(3)	1/2	0.62	0.0050(4)	0.0012(1)	0.0023(1)	0.0	0.0000(2)	0.0
T(1)	0.0745(2)	0.1688(3)	0.2276(1)	0.52	0.0053(3)	0.0010(1)	0.0016(1)	0.0003(1)	0.0003(1)	-0.00015(7)
T(11)	0.5844(2)	0.3323(3)	0.2275(1)	0.54	0.0044(3)	0.0009(1)	0.0022(1)	0.0002(1)	0.0006(1)	-0.00003(8)
O(1)	0.0289(6)	-0.0002(5)	0.1720(3)	1.40	0.0202(9)	0.0021(2)	0.0030(2)	-0.0000(6)	0.0002(3)	-0.0002(3)
O(2)	0.3248(7)	0.2350(5)	0.1725(4)	1.42	0.0125(9)	0.0053(3)	0.0029(3)	-0.0031(5)	0.0019(4)	-0.0005(3)
O(22)	0.8177(7)	0.2641(5)	0.1597(4)	1.34	0.0117(9)	0.0046(3)	0.0031(3)	0.0028(4)	0.0010(4)	0.0007(2)
O(3)	0.1155(6)	0.1748(4)	0.3939(3)	0.71	0.0067(7)	0.0019(2)	0.0019(2)	0.0011(3)	0.0008(3)	-0.0001(2)
O(33)	0.6639(5)	0.3271(5)	0.3928(3)	0.75	0.0058(6)	0.0022(2)	0.0022(2)	0.0002(4)	0.0003(3)	0.0000(2)
F(1)	0.1089(5)	0.4715(3)	0.3989(3)	1.10	0.0108(7)	0.0025(2)	0.0032(2)	-0.0007(3)	0.0009(3)	0.0005(2)

$B_{\text{equiv.}}$ calculated from anisotropic data according to Hamilton (1959). The anisotropic temperature factor form is $\exp(-\sum_i \Sigma_j \beta_i h_j h_j)$.

The size and scattering power of $M(2)$ are consistent with complete ordering of Al into this site. To a first approximation, the remaining octahedral cations and vacancies of the formula unit can be considered randomly distributed over $M(1)$ and $M(3)$. For this random distribution the distance of the average cation from its oxygen neighbors, neglecting the (F,OH) contacts, was calculated from the radii of Shannon and Prewitt (1969, 1970) as 2.133 Å. The size of a vacancy was taken as 0.80 Å in this calculation. The observed values from Table 4 are 2.133 Å for mean $M(1)$ —O and 2.117 Å for mean $M(3)$ —O. A better overall fit for calculated sizes and electron counts is obtained by moving all the smaller and lighter Al out of $M(1)$ into $M(3)$ and replacing with a corresponding amount of Fe^{2+} . The calculated M —O values then become 2.140 Å for $M(1)$ and 2.127 Å for $M(3)$, and the calculated electron counts become 13.9 and 13.1, respectively. Despite the good fit, this should not be considered a unique solution.

The (F,OH) atom has a high temperature factor ($B = 3.0 \text{ \AA}^2$) when refined in $C2/m$ symmetry. Figure 1 shows that in $C2$ symmetry the (F,OH) atom has moved off the mirror plane to coordinate more closely with Al in $M(2)$. At the same time the equivalent isotropic B value for (F,OH) has decreased to 1.1 Å^2 (Table 3). The $M(3)$ —(F,OH) distance of 2.159 Å (Table 4) is larger than the $M(3)$ —O distances (2.109, 2.125 Å). This octahedral irregularity, to be discussed in more detail below, was the reason for using only the oxygen contacts in calculating the octahedral cation distributions mentioned in the preceding paragraph.

The (F,OH) atom is located in the *trans*-orienta-

tion at opposite apices of the $M(1)$ octahedron but in the *cis*-orientation along a shared edge between the $M(2)$ and $M(3)$ octahedra (Fig. 1). Because fluorine is smaller than oxygen, two (F,OH) atoms can approach each other more closely along the shared edge between $M(2)$ and $M(3)$ than can two oxygens along any $M(1)$ shared edge. Thus, the smaller Al can be accommodated more readily in either $M(2)$ or $M(3)$ than in $M(1)$. The small amount of tetrahedral ordering present in this crystal also favors location of a high-charge cation in $M(2)$. The shared octahedral edge between $M(2)$ and $M(1)$ that parallels the F—F shared edge between $M(2)$ and $M(3)$ involves two O(3) atoms apical to $T(1)$ cations in the upper and lower tetrahedral sheets (Fig. 1). Because of Al concentration in $T(1)$, the apical O(3) anions are undersaturated and thus favor a trivalent cation in $M(2)$. Reversal of the tetrahedral ordering pattern by placing more Al^{IV} in $T(11)$ would favor octahedral Al in $M(3)$ instead of $M(2)$, and the particular pattern adopted may be a random choice from crystal to crystal. This also may lead to domain structures. It is anticipated that the O—H dipole will be deflected from the sheet normal to point away from $M(2)$ in a direction between $M(1)$ and $M(3)$ and toward the undersaturated O(3)—O(3) shared edge of the next $M(2)$ octahedron.

Ordering model

Rieder (1968) was correct in predicting that zinnwaldite would show octahedral ordering, although the observed ordering pattern is rotated 120° from that predicted. Rieder emphasized the smaller $d(001)$ values of natural zinnwaldites relative to synthetic

Table 4. Calculated bond lengths and angles

Bond lengths (Å)			Bond angles (°)	
Tetrahedron T(1)				
0(1)	1.646(4)	0(1)--0(2)	2.655(5)	0(1)--0(2)
0(2)	1.640(4)	0(22)	2.653(5)	0(22)
0(22)	1.646(4)	0(3)	2.721(4)	0(3)
0(3)	1.653(4)	0(2)--0(22)	2.664(6)	0(2)--0(22)
Mean	1.646	0(3)	2.727(5)	0(3)
		0(22)--0(3)	2.706(5)	0(22)--0(3)
		Mean	2.688	Mean
				107.8(2)
				107.4(2)
				111.1(2)
				108.3(2)
				111.8(2)
				110.2(2)
				109.4
Tetrahedron T(11)				
0(1)	1.637(4)	0(1)--0(2)	2.649(5)	0(1)--0(2)
0(2)	1.639(4)	0(22)	2.654(5)	0(22)
0(22)	1.638(4)	0(3)	2.715(4)	0(3)
0(33)	1.643(3)	0(2)--0(22)	2.638(6)	0(2)--0(22)
Mean	1.639	0(3)	2.712(5)	0(3)
		0(22)--0(33)	2.692(5)	0(22)--0(33)
		Mean	2.677	Mean
				107.9(2)
				108.2(2)
				111.7(2)
				107.2(2)
				111.4(2)
				110.2(2)
				109.4
Interlayer cation K(1)			T(1) to T(11)	
0(1)x2	2.994(3)	3.286(3)	around 0(1)	139.1(2)
0(2)x2	2.999(4)	3.291(5)	around 0(2)	139.4(2)
0(22)x2	2.978(4)	3.177(4)	around 0(22)	130.5(2)
Mean	2.990	3.251	Mean	136.3
	(inner)	(outer)		
Octahedron M(1)				
0(3)x2	2.127(4)		0(3)--0(33)x2	96.8(1)
0(33)x2	2.138(4)		F(1)x2	100.0(1)
F(1)x2	2.130(3)		0(33)--F(1)x2	97.9(1)
Mean	2.132		Mean (unshared)	98.2
0(3)--0(33)x2	3.189(4)		0(3)--0(3)	77.3(2)
F(1)x2	3.261(4)		F(1)x2	88.3(1)
0(33)--F(1)x2	3.219(4)		0(33)--0(33)	89.6(2)
Mean (unshared)	3.223		F(1)x2	74.4(1)
0(3)--0(3)	2.656(6)		Mean (shared)	82.1
F(1)x2	2.967(4)			
0(33)--0(33)	3.013(6)			
F(1)x2	2.579(4)			
Mean (shared)	2.794			
Octahedron M(2)				
0(3)x2	1.889(4)		0(3)--0(33)x2	93.5(1)
0(33)x2	1.895(3)		F(1)x2	92.6(1)
F(1)x2	1.862(3)		0(33)--F(1)x2	91.1(1)
Mean	1.882		Mean (unshared)	92.4
0(3)--0(33)x2	2.755(4)		0(3)--0(3)	89.4(2)
F(1)x2	2.712(3)		0(33)x2	88.6(1)
0(33)--F(1)x2	2.681(4)		0(33)--F(1)x2	86.7(1)
Mean (unshared)	2.716		F(1)--F(1)	85.4(2)
0(3)--0(3)	2.656(6)		Mean (shared)	87.6
0(33)x2	2.643(4)			
0(33)--F(1)x2	2.579(4)			
F(1)--F(1)	2.524(5)			
Mean (shared)	2.604			
Octahedron M(3)				
0(3)x2	2.109(3)		0(3)--0(33)x2	98.6(1)
0(33)x2	2.125(4)		F(1)x2	96.7(1)
F(1)x2	2.159(3)		0(33)--F(1)x2	99.3(1)
Mean	2.131		Mean (unshared)	98.2
0(3)--0(33)x2	3.209(4)		0(3)--0(33)x2	77.3(1)
F(1)x2	3.189(4)		F(1)x2	88.1(1)
0(33)--F(1)x2	3.265(4)		0(33)--0(33)	90.3(2)
Mean (unshared)	3.221		F(1)--F(1)	71.5(1)
0(3)--0(33)x2	2.643(4)		Mean (shared)	82.1
F(1)x2	2.967(4)			
0(33)--0(33)	3.013(6)			
F(1)--F(1)	2.524(5)			
Mean (shared)	2.793			

specimens as evidence for ordering, and also noted that the natural specimens were more F-rich than the synthetic specimens, which were grown in equilibrium with a buffer of low fluorine fugacity. The difference of 0.1 Å noted in the $d(001)$ values by Rieder

probably is due primarily to the presence of fluorine. Calculation of the octahedral sheet thickness in the present study by considering the apical oxygens separately from the (F,OH) atom does result in a difference of 0.1 Å. In addition, Yoder and Eugster (1954) showed a decrease in basal spacing of 0.18 Å for fluorophlogopite relative to hydroxyphlogopite, where octahedral ordering cannot be a factor. It should be noted also that the clintonite-1M (xanthophyllite), the model for the Rieder ordering pattern, actually has an octahedral sheet not appreciably different in thickness (2.148 Å) than for disordered F-poor trioctahedral micas (range 2.09–2.22 Å).

We suggest that the ordering pattern observed in this study, namely with the small cation in either $M(2)$ or $M(3)$, should be found in all F-rich zinnwaldites and lepidolites. Some evidence for this view can be found in the anomalously high B values for the (F,OH) atom in micas that show the "normal" ordering pattern, with $M(1)$ larger than the average $M(2,3)$ atom, but that have not been refined in subgroup symmetry, namely $B = 2.78 \text{ Å}^2$ in fluor-polyolithionite-1M (Takeda and Burnham, 1969), $B = 2.92$ and 1.77 Å^2 in lepidolite-2M₂ (Takeda *et al.*, 1971; Sartori *et al.*, 1973), and $B = 2.32 \text{ Å}^2$ in lepidolite-1M (Sartori, 1976). Additional evidence comes from the cell dimensions of zinnwaldites. Bailey (1975) has shown that the "normal" ordering pattern necessarily gives rise to an intralayer shift larger than the ideal value of $-a/3$ and, unless compensated by an offset of adjacent layers, to an observed β angle for 1M micas larger than ideal. It is possible to obtain values of $\text{csin}\beta$, a , and β for 11 zinnwaldites from graphs presented by Rieder (1968, 1970b) and Rieder *et al.* (1971). In all cases the "normal" ordering pattern is predicted, including specimen # 40 whose structure is presented here ($\beta_{\text{obs}} = 100.83^\circ$, $\beta_{\text{ideal}} = 100.07^\circ$). For three synthetic annites the observed and ideal β angles are approximately equal, as should be true where the octahedra are of similar sizes.

Structural distortions

Important structural features of zinnwaldite-1M are summarized in Table 5. Tetrahedra $T(1)$ and $T(11)$ are similar in shape, only slightly elongate, and rotated by 5.8° . The small octahedron $M(2)$ containing Al is nearly regular in shape, but $M(1)$ and $M(3)$ are considerably flattened and distorted (Fig. 1). The individual ψ values of 60.8° (ideal = 54.73°) for $M(1)$ and $M(3)$ are among the largest recorded for micas to date, and are a measure of the amount of flattening required to fit these large Fe,Li-rich octahedra onto

Table 5. Important structural features of zinnwaldite

Parameter	Value
a_{tet}^{α} (°)	5.8
b_{tet}^{τ} (°)	T(1): 111.0 T(11): 111.1
e_{ideal}^{β} (°)	100.07
c, d_{ψ}^{oct} (°)	M(1), M(3): 60.8 M(2): 56.5 Mean: 59.5
$d_{\text{sheet thickness}}^{\text{tetrahedral}}$ (Å)	2.252
$d_{\text{sheet thickness}}^{\text{octahedral}}$ (Å)	2.078
Interlayer separation (Å)	3.333
Basal oxygen Δz_{ave} (Å)	0.124
Intralayer shift	-0.354a ₁
Layer offset	-0.004a ₁
Resultant shift	-0.358a ₁

^aTetrahedral rotation is calculated from $\alpha = 1/2|120^\circ - \text{mean } O_b-O_b-O_b \text{ angle}|$.

^bThe tetrahedral angle is defined as $\tau = O_{\text{apical}}-T-O_{\text{basal}}$. The ideal value is 109.47°.

^cThe mean octahedral angle, ideally 54.73°, is calculated from $\cos\psi = \text{oct. thickness}/2(M-O, F, OH)$.

^dIncludes the position of F(1) in the calculation.

$e_{\text{ideal}}^{\beta} = 180^\circ - \cos^{-1}(a/3c)$.

the adjacent smaller and thinner octahedron ($\psi = 56.5^\circ$) around the Al in M(2). The sheet thicknesses are similar to those found in other F-rich trioctahedral micas.

Apparent thermal vibrations

Tables 6 and 7 list the orientations of the thermal ellipsoids and the calculated bond lengths after correction for thermal effects. The apparent thermal motions of zinnwaldite resemble those of phlogopite (and annite) in some aspects and are unique in others. Like phlogopite, the apparent thermal motions are large in both magnitude and anisotropy. Hazen and Burnham (1973) suggest that such apparent thermal motions are due, in part, to local variations in atomic positions. Also like phlogopite, equivalent isotropic temperature factors of the apical oxygens [O(3) and O(33)] are considerably smaller in magnitude than those of the basal oxygens. These differences in thermal magnitudes may be related to the differences in bond lengths between tetrahedral Al and Si and to lack of appreciable tetrahedral order. The basal oxygens are coordinated to two tetrahedra and are, therefore, more affected by the different Si—O and Al^{IV}—O bond lengths than are the apical oxygens.

In phlogopite most of the atoms are elongate along

Z*. In zinnwaldite the elongation is along Z* and Z. However, some atoms also appear to be elongate along the bonds to them. Most significantly, the (F,OH) atom is elongate along the bonds to both M(1) and M(3), and this suggests a small amount of positional disorder for (F,OH). NMR studies of phlogopites with varying amounts of F and OH indicate (1) a tendency for F—F pairing along the same octahedral edge rather than a random distribution, and (2) preferential location of Fe²⁺ in sites close to OH groups (Sanz and Stone, 1977.) This is in accord also with the known preference of Al for F rather than for OH, as summarized by Kampf (1977). It is interesting to note in the Sadisdorf zinnwaldite specimen that OH makes up 39 percent of the F,OH total and that Fe²⁺ also makes up 39 percent of the total occupancy of M(1) + M(3). This may indicate a local clustering or domain structure, in which 39 percent of the volume of the crystal consists of OH—OH pairs located closer to Fe²⁺ in M(1) and M(3) than to Al in M(2), and 61 percent consists of F—F pairs located

Table 6. Orientations of thermal ellipsoids relative to crystal axes

Atom	Axis	rms (Å) displacement	Angle (°) with respect to		
			X	Y	Z
K(1)	r ₁	0.143(2)	90	0	90
	r ₂	0.156(2)	150(6)	90	109(6)
	r ₃	0.168(2)	120(6)	90	19(6)
M(1)	r ₁	0.062(4)	90	0	90
	r ₂	0.091(2)	163(5)	90	62(5)
	r ₃	0.110(2)	73(5)	90	28(5)
M(2)	r ₁	0.078(4)	90	0	90
	r ₂	0.082(3)	178(13)	90	77(13)
	r ₃	0.093(4)	88(13)	90	13(13)
M(3)	r ₁	0.071(5)	90	0	90
	r ₂	0.080(3)	156(5)	90	103(5)
	r ₃	0.110(3)	114(5)	90	13(5)
T(1)	r ₁	0.063(4)	102(5)	14(4)	80(4)
	r ₂	0.084(3)	145(11)	95(6)	113(12)
	r ₃	0.094(3)	122(11)	103(4)	25(11)
T(11)	r ₁	0.061(4)	100(8)	10(8)	88(3)
	r ₂	0.078(3)	169(7)	100(8)	84(4)
	r ₃	0.104(3)	94(4)	91(3)	7(4)
O(1)	r ₁	0.095(5)	89(4)	7(13)	83(12)
	r ₂	0.121(4)	99(3)	83(13)	159(5)
	r ₃	0.171(4)	9(3)	89(4)	110(3)
O(2)	r ₁	0.106(6)	145(7)	118(9)	62(21)
	r ₂	0.117(6)	99(19)	111(11)	151(21)
	r ₃	0.167(5)	123(4)	36(4)	97(5)
O(22)	r ₁	0.102(6)	132(7)	53(4)	106(10)
	r ₂	0.127(6)	61(9)	94(9)	161(10)
	r ₃	0.157(5)	56(5)	37(4)	82(7)
O(3)	r ₁	0.076(6)	130(8)	41(8)	76(12)
	r ₂	0.098(5)	96(22)	86(18)	162(18)
	r ₃	0.106(5)	40(9)	50(8)	100(25)
O(33)	r ₁	0.087(5)	26(18)	106(26)	81(11)
	r ₂	0.097(5)	105(26)	164(27)	93(27)
	r ₃	0.107(5)	110(12)	90(26)	9(12)
F(1)	r ₁	0.096(5)	72(7)	25(5)	110(5)
	r ₂	0.121(4)	145(12)	84(9)	113(13)
	r ₃	0.134(4)	118(13)	66(5)	31(10)

Table 7. Bond lengths corrected for thermal motion

Bond	Distance (Å)		Bond	Distance (Å)	
	Correlation high	Correlation none		Correlation high	Correlation none
M(1) octahedron					
0(3)x2	2.128(4)	2.136(4)			
0(33)x2	2.140(4)	2.148(4)			
F(1)x2	2.142(3)	2.149(3)			
Mean	2.137	2.144			
0(3)-0(3)	2.660(6)	2.667(6)	0(3)-0(33)x2	3.189(4)	3.195(4)
F(1)x2	2.971(4)	2.977(4)	F(1)x2	3.275(4)	3.279(4)
0(33)-0(33)	3.019(6)	3.025(6)	0(33)-F(1)x2	3.220(4)	3.226(4)
F(1)x2	2.583(4)	2.590(4)	Mean	3.228	3.233
Mean (shared)	2.798	2.804	(unshared)		
M(2) octahedron					
0(3)x2	1.890(4)	1.898(4)			
0(33)x2	1.896(3)	1.904(3)			
F(1)x2	1.866(3)	1.874(3)			
Mean	1.884	1.892			
0(3)-0(3)	2.660(6)	2.667(6)	0(3)-0(33)x2	2.755(4)	2.762(4)
0(33)x2	2.645(4)	2.652(4)	F(1)x2	2.714(3)	2.721(3)
0(33)-F(1)x2	2.583(4)	2.590(4)	0(33)-F(1)x2	2.683(4)	2.690(4)
F(1)-F(1)	2.527(5)	2.537(5)	Mean	2.717	2.724
Mean (shared)	2.607	2.615	(unshared)		
M(3) octahedron					
0(3)x2	2.109(3)	2.117(3)			
0(33)x2	2.126(4)	2.133(4)			
F(1)x2	2.161(3)	2.169(3)			
Mean	2.132	2.140			
0(3)-0(33)x2	2.645(4)	2.652(4)	0(3)-0(33)x2	3.210(4)	3.215(4)
F(1)x2	2.971(4)	2.977(4)	F(1)x2	3.189(4)	3.196(4)
0(33)-0(33)	3.019(6)	3.025(6)	0(33)-F(1)x2	3.267(4)	3.273(4)
F(1)-F(1)	2.527(5)	2.537(5)	Mean	3.222	3.228
Mean (shared)	2.796	2.803	(unshared)		
T(1) tetrahedron					
0(1)	1.655(4)	1.664(4)	0(1)-0(2)	2.660(5)	2.674(5)
0(2)	1.649(4)	1.656(4)	0(22)	2.655(5)	2.670(5)
0(22)	1.654(4)	1.663(4)	0(3)	2.717(4)	2.732(4)
0(3)	1.654(4)	1.661(4)	0(2)-0(22)	2.664(6)	2.677(6)
Mean	1.653	1.661	0-(3)	2.723(5)	2.738(5)
			0(22)-0(3)	2.702(5)	2.716(5)
			Mean	2.687	2.701
T(11) tetrahedron					
0(1)	1.645(4)	1.655(4)	0(1)-0(2)	2.650(5)	2.666(5)
0(2)	1.647(4)	1.656(4)	0(22)	2.659(5)	2.673(5)
0(22)	1.645(4)	1.654(4)	0(33)	2.711(4)	2.726(4)
0(33)	1.645(3)	1.651(3)	0(2)-0(22)	2.637(6)	2.652(6)
Mean	1.646	1.654	0(3)	2.708(5)	2.722(5)
			0(22)-0(33)	2.688(5)	2.701(5)
			Mean	2.676	2.690
Interlayer cation K(1)					
0(1)x2	2.991(3)	3.007(3)			
0(2)x2	2.997(4)	3.013(4)			
0(22)x2	2.975(4)	2.991(4)			
Mean (inner)	2.988	3.004			
0(1)x2	3.294(3)	3.307(3)			
0(2)x2	3.292(5)	3.307(5)			
0(22)x2	3.177(4)	3.193(4)			
Mean (outer)	3.254	3.269			

closer to Al in $M(2)$ than to Li and the remaining cations in $M(1)$ and $M(3)$. Under this interpretation the bulk of the thermal ellipsoid of (F,OH) is determined by the positions of the F (61 percent), and the elongation toward $M(1)$ and $M(3)$ is produced by the closer approach of the OH (39 percent) to the Fe in those sites. In addition to the elongation of (F,OH) along the $M(1)$ and $M(3)$ bonds, the $M(1)$ site is observed to be elongate along the $M(1)$ —(F,OH) bond.

Acknowledgments

We thank the donors of the Petroleum Research Fund, administered by the American Chemical Society, for partial support of this research by grant 8425-AC2 and to the National Science Foundation for partial support through grants GA-34918 and EAR76-06620. We also thank Dr. Milan Rieder of Charles University for providing the zinnwaldite crystal used in this study. Mr. Darrell J. Henry of the University of Wisconsin for the electron microprobe analysis, Dr. Wayne A. Dollase of UCLA for use of program OPTDIS, and Dr. Werner H. Baur of the University of Illinois at Chicago Circle for advice on refinement procedures.

References

- Bailey, S. W. (1975) Cation ordering and pseudosymmetry in layer silicates. *Am. Mineral.*, **60**, 175-187.
- Foster, M. D. (1960) Interpretation of the composition of lithium micas. *U.S. Geol. Surv. Prof. Pap.*, **354-E**, 115-147.
- Guggenheim, S. and S. W. Bailey (1975) Refinement of the margarite structure in subgroup symmetry. *Am. Mineral.*, **60**, 1023-1029.
- Hamilton, W. C. (1959) On the isotropic temperature factor equivalent to a given anisotropic temperature factor. *Acta Crystallogr.*, **12**, 609-610.
- (1965) Significance tests on the crystallographic R factor. *Acta Crystallogr.*, **18**, 502-510.
- Hazen, R. M. and C. W. Burnham (1973) The crystal structures of one-layer phlogopite and annite. *Am. Mineral.*, **58**, 889-900.
- Kampf, A. R. (1977) Minyulite: its atomic arrangement. *Am. Mineral.*, **62**, 256-262.
- Rieder, M. (1968) Zinnwaldite: octahedral ordering in lithium-iron micas. *Science*, **160**, 1338-1340.
- (1970a) Chemical composition and physical properties of lithium-iron micas from the Krušné hory Mts. (Erzgebirge). Part A. Chemical composition. *Contrib. Mineral. Petrol.*, **27**, 131-158.
- (1970b) Lithium-iron micas from the Krušné hory Mountains (Erzgebirge): Twins, epitaxial overgrowths and polytypes. *Z. Kristallogr.*, **132**, 161-184.
- , A. Píčová, M. Fassová, E. Fediuková, and P. Černý (1971) Chemical composition and physical properties of lithium-iron micas from the Krušné hory (Erzgebirge), Czechoslovakia and Germany. Part B: Cell parameters and optical data. *Mineral. Mag.*, **38**, 190-196.
- Sanz, J. and W. E. E. Stone (1977) Order-disorder in the octahedral layer of phlogopites: an investigation by NMR (abstr.). *Proc. 3rd European Clay Conf., Oslo*, 167-169.

- Sartori, F. (1976) the crystal structure of a 1*M* lepidolite. *Tschermaks Mineral. Petrogr. Mitt.*, 23, 65-75.
- , M. Franzini and S. Merlino (1973) Crystal structure of a 2*M*₂ lepidolite. *Acta Crystallogr.*, B29, 573-578.
- Shannon, R. D. and C. T. Prewitt (1969) Effective ionic radii in oxides and fluorides. *Acta Crystallogr.*, B25, 925-946.
- (1970) Revised values of effective ionic radii. *Acta Crystallogr.*, B26, 1046-1048.
- Sidorenko, O. V., B. B. Zvyagin and S. V. Soboleva (1975) Crystal structure refinement for 1*M* dioctahedral mica. *Soviet Physics-Crystallogr.*, 20, 332-335 (English transl.).
- Takeda, H. and C. W. Burnham (1969) Fluor-polyolithionite: a lithium mica with nearly hexagonal (Si₂O₅)²⁻ ring. *Mineral. J. (Japan)*, 6, 102-109.
- , N. Haga and R. Sandanaga (1971) Structural investigation of polymorphic transition between 2*M*₂-, 1*M*-lepidolite and 2*M*₁ muscovite. *Mineral. J. (Japan)*, 6, 203-215.
- Yoder, H. S. and H. P. Eugster (1954) Phlogopite synthesis and stability range. *Geochim. Cosmochim. Acta*, 6, 157-185.

*Manuscript received, February 7, 1977; accepted
for publication, June 20, 1977.*